Core Follow Calculation for Hanbit Unit 3 using DeCART2D/MASTER

Sungmin Kim*, Cheonbo Shim, Yonghee Choi and Kyunghoon Lee

Korea Atomic Energy Research Institute, 111, Daedeok-daero 989beon-gil, Yuseong-gu, Daejeon, 34057, Korea
*Corresponding author: smkim0921@kaeri.re.kr

1. Introduction

Korea Atomic Energy Research Institute (KAERI) has developed the two-step procedure based the DeCART2D [1]/MASTER4.0 [2] code system for the nuclear design. MASTER4.0 is rewriting version of MASTER3.0 [3] and maintains most of all capabilities of MASTER3.0. Module of MASTER4.0 based derived type variables. Moreover, MASTER4.0 has neutronics solution methods of the Source Expansion Nodal Method (SENM) for a rectangular geometry and the Triangle based Polynomial Expansion Nodal (TPEN) method for a hexagonal geometry. In addition, depletion of MASTER4.0 based on Krylov subspace method. DeCART2D that is a neutron transport code based on Method of Characteristic (MOC) has developed to generate assembly-wise homogenized group constants (HGCs) used in nodal diffusion core analysis codes such as MASTER for a two-step procedure. MASTER is a neutron diffusion nodal code for a nuclear design of PWRs and it has the capabilities to analyze the steady-state and transient core behaviors in 3-D geometry based on the two-group diffusion theory.

As a part of code system verification and validation (V&V) for DeCART2D/MASTER4.0, a core follow calculation for Hanbit Unit 3 in cycle 1 was performed. The computed results are then compared to the measured reference data as well as computed data generated by CASMO-3/MASTER3.0.

2. Methods and Results

2.1 Generation of MASTER Cross Section Library

In order to perform core follow calculation using MASTER, HGC data from DeCART2D should be generated and converted to the suitable library format available in MASTER. HGC data are three types that fuel assemblies (FAs), radial reflectors and axial reflectors, respectively.

There are nine types of fuel assembly loaded in Hanbit Unit 3 in cycle 1. In addition, cutback and in-core detector region should be considered for fuel assembly modelling. Therefore, twenty-three types of fuel assemblies were modeled for FA HGC data generation. Fig. 1 presents the sample of 1/8 rotational FA.
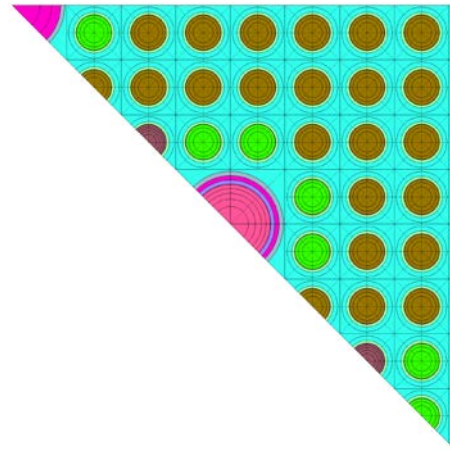

Fig. 1. Radial fuel configuration of fuel assembly

The radial reflector region for Hanbit Unit 3 core consists of the core shroud, moderator and the core support barrel. Fig. 2 shows the radial reflector model in order to generate radial reflector HGC data. Note that HGC of radial reflector nodes are generated simultaneously by solving the 2-D core problem in the DeCART2D/MASTER4.0 code system instead of adopting the simple FA/reflector two-node model used in various lattice codes such as CASMO-3. The 2-D core model is expected to predict the precise neutron spectrum and flux distribution at the reflector nodes compared to the conventional two-node model.
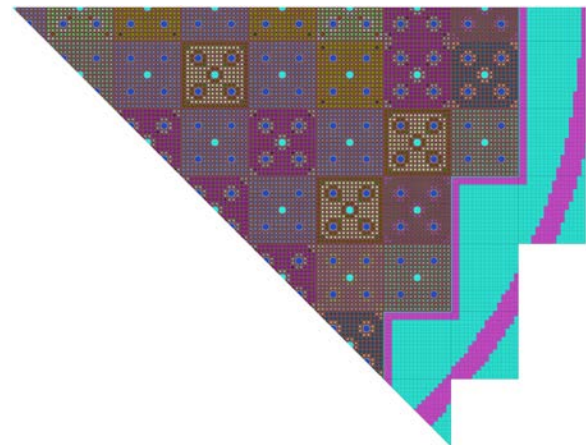

Fig. 2. Radial reflector model of Hanbit Unit 3

In general, the FA-reflector two-node method has been used to generate radial as well as axial reflector HGC data. However, this method cannot consider the actual flux shape at the interface between the FAs and reflector. In this paper, a simplified 1-D model is used to generate axial reflector HGC data instead of using the

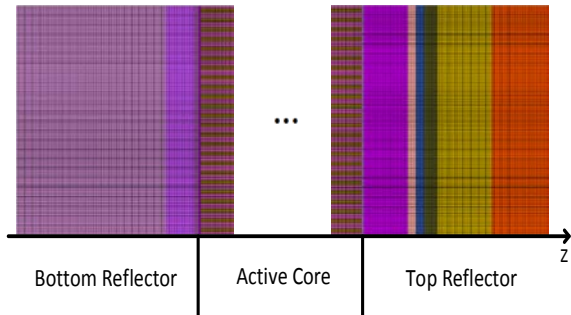two-node model for more realistic modelling [4]. Fig. 3 shows the simplified 1-D axial reflector model.

Fig. 3. Simplified 1-D axial reflector model

PROLOG [5] and PROMARX [4] codes are used to convert HGC data of fuel assemblies and reflectors to MASTER cross section library format, respectively.

2.2 Core Follow Calculation

A core follow calculation for Hanbit Unit 3 in cycle 1 was performed using DeCART2D/MASTER4.0. The core loading pattern, control rod map, location of in-core detectors, axial core configuration, core operating history and other core conditions are applied to make the MASTER core follow analysis input model. The results of core follow calculation were compared to the measured and computed reference data. These comparisons include critical boron concentration (CBC), inverse boron worth (IBW), control rod worth (CRW), isothermal temperature coefficient (ITC) and power coefficient (PC).

2.3 Results

In this paper, the reference data means the measured value and computed data from CASMO-3/MASTER3.0. Fig. 4 shows the reference and computed CBCs at each burnup steps and Fig. 5 shows the reactivity error between calculated and measured values. DeCART2D/MASTER4.0 CBC curve is very consistent with reference data.
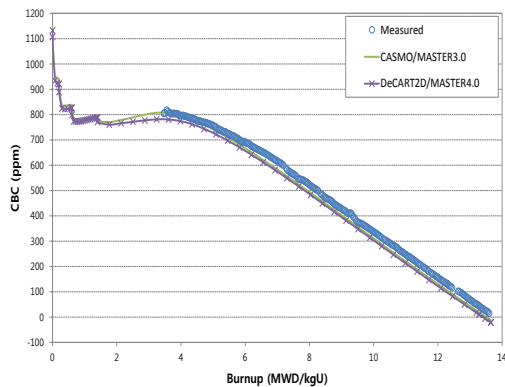

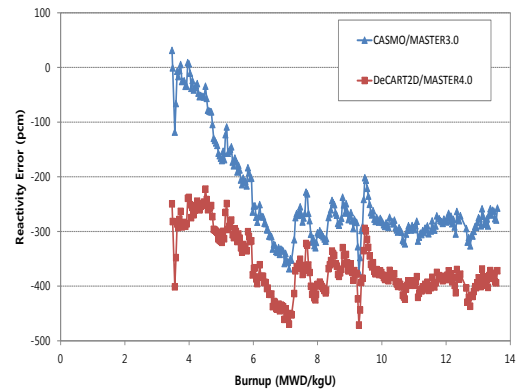Fig. 4. Comparison of reference and computed CBCs.

Fig. 5. Error in reactivity

Table I shows the differences between measured and computed IBWs. In Table I, the number 1 through 5 is the index for regulating control bank.

Table I: Differences between measured and computed IBWs

Condition	Deviation (ppm/pcm)		
	C-M	D-M	D-C
CZP 5+4+3+2+1	0.0005	0.0027	0.0022
HZP 5+4+3	-0.0003	0.0015	0.0018

M: Measured
C: CASMO-3/MASTER3.0
D: DeCART2D/MASTER4.0

Table II and Table III present the differences between measured and computed CRWs at CZP and HZP conditions, respectively. In Table II, the inserted bank A means the shutdown bank A. The maximum differences are -8.27 % and -9.32 % at CZP and HZP conditions, respectively. Also, these differences were presented Fig. 6 and Fig. 7. The actual CRW values are not specified in this paper.

Table II: Differences between measured and computed CRWs at CZP

CZP Condition			
Inserted Bank	Deviation (%)		
	(C-M)/M	(D-M)/M	(D-C)/M
5	-14.29	-8.27	6.02
5+4	-6.63	1.06	7.69
5+4+3	-3.67	2.97	6.64
5+4+3+2	-1.27	6.22	7.50
5+4+3+2+1	-3.33	3.21	6.54
5+4+3+2+1+A	-5.95	0.29	6.23

Table III: Differences between measured and computed CRWs at HZP

HZP Condition			
Inserted Bank	Deviation (%)		
	(C-M)/M	(D-M)/M	(D-C)/M
5	-10.19	-9.32	0.87
5+4	-3.27	-1.78	1.49
5+4+3	-1.44	-0.54	0.90
5+4+3+2	-0.24	1.01	1.24
5+4+3+2+1	-2.38	-1.28	1.10

Table IV: Differences between measured and computed ITCs

Condition	Deviation (ppm/°C)		
	C-M	D-M	D-C
HZP ARO	1.13	-0.16	-1.29
20%P ARO	-0.34	-2.24	-1.90
50%P ARO	-0.82	-2.51	-1.68
80%P ARO	-1.58	-3.09	-1.51
95%P ARO	-1.18	-2.98	-1.80
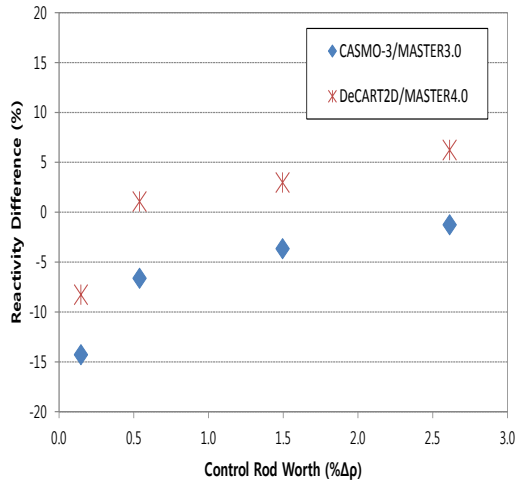
Fig. 6. Difference in control rod worth at CZP condition

Fig. 8. Difference in Isothermal temperature coefficient

Table V shows the differences of PC at each reactor power condition between measured and computed values. These conditions are 20%P, 50%P, 80%P and 95%P, respectively. These results are presented in Fig. 9, also. The maximum difference between measured and computed PCs is 0.85 pcm/%P.

Table V: Differences between measured and computed PCs

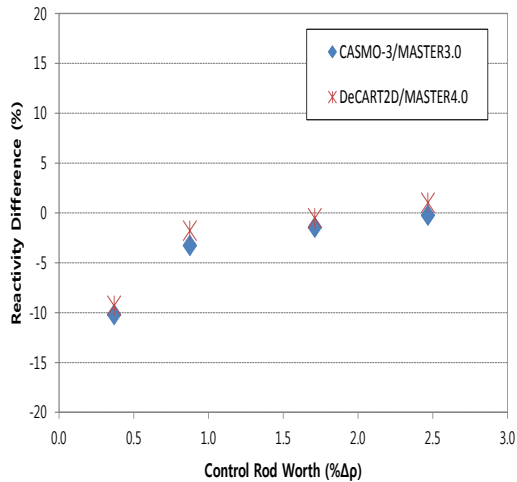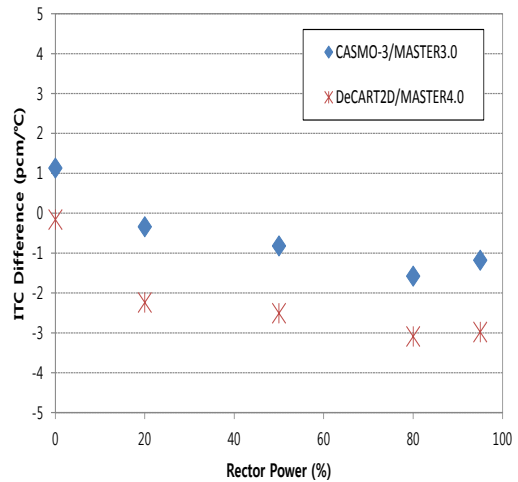| Condition	Deviation (ppm/%power)		
	C-M	D-M	D-C
20%P ARO	0.65	0.40	-0.25
50%P ARO	0.40	-0.07	-0.47
80%P ARO	-0.22	-0.85	-0.63
95%P ARO	0.38	-0.43	-0.80

Fig. 7. Difference in control rod worth at HZP condition

The differences between measured values and computed data in ITC at each reactor power condition are shown in Table IV. The comparisons were performed at ARO conditions and the reactor power condition of each case is HZP, 20%P, 50%P, 80%P and 95%P, respectively. The maximum difference between measured values and computed data is -3.09 pcm/°C. Fig. 8 shows the differences between measured values and computed data in ITCs.
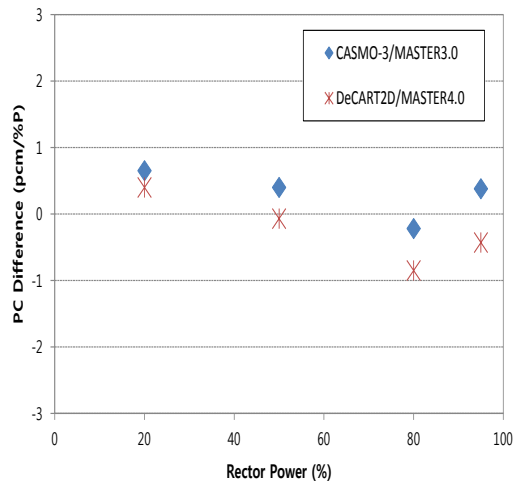

Fig. 9. Difference in power coefficient

3. Conclusions

In the paper, a core follow calculation for Hanbit Unit 3 in cycle 1 was performed using the DeCART2D/MASTER4.0 nuclear design code system developed in KAERI. Three types HGC data were generated using the DeCART2D code and PROLOG and PROMARX converted these HGC for available in MASTER code. Various nuclear parameters such as CBC, IBW, CRW, ITC and PC were generated by DeCART2D/MASTER4.0 and they are compared to the measured data and CASMO-3/MASTER3.0 results. Although some parameters have relatively large uncertainty compared to CASMO-3/MASTER3.0, most data have good agreement with the reference measured data. As a result, it can be concluded that DeCART2D/MASTER4.0 has sufficient capabilities for nuclear designs.

REFERENCES

[1] J. Y. Cho, et al., "DeCART2D v1.1 User's Manual," KAERI/UM-40/2016, 2016.
[2] J. Y. Cho, et al., "MASTER v4.0 User's Manual," KAERI/UM-41/2016, 2016.
[3] J. S. Song, et al., "Verification and Uncertainty Evaluation of CASMO-3/MASTER Nuclear Analysis System," KAERI/TR-806/97, 1997.
[4] C. B. Shim, et al., "Improvement of Axial Reflector Cross Section Generation Model for PWR Core Analysis," Transactions of the Korean Nuclear Society Autumn Meeting, Gyeongju, Korea, October 27-28, 2016.
[5] J. S. Song, et al., "PROLOG1.1 User's Manual," KAERI/UM-4/99, 1999.